DOI:10.1021/jf903216r

JOURNAL OF AGRICULTURAL AND FOOD CHEMISTRY
ARTICLE

Anticancer Effects of Flavonoid Derivatives Isolated from *Millettia reticulata* Benth in SK-Hep-1 Human Hepatocellular Carcinoma Cells

Song-Chwan Fang,[†] Chin-Lin Hsu,[‡] Hsin-Tang Lin,[§] and Gow-Chin Yen*,[∥]

[†]Department of Food Nutrition, Chung Hwa University of Medical Technology, 89 Wenhwa First Street, Tainan 71703, Taiwan, [‡]School of Nutrition, Chung Shan Medical University, No. 110, Section 1, Jianguo North Road, Taichung 40201, Taiwan, [§]Department of Food Science, Nutrition and Nutraceutical Biotechnology, Shih Chien University, No. 70 Ta-Chih Street, Taipei 10462, Taiwan, and [∥]Department of Food Science and Biotechnology, National Chung Hsing University, 250 Kuokuang Road, Taichung 40227, Taiwan

Millettia reticulata Benth is cultivated in Asian countries. *M. reticulata* Benth has multiple biological functions and is one of the oldest tonic herbs in traditional Chinese medicine. It has been elevated to one of the most commonly used herbs in modern Chinese medicine. The aims of this work were to study the in vitro anticancer activity of flavonoid derivatives isolated from the stems of *M. reticulata* Benth. Six flavonoid derivatives including (−)-epicatechin (**1**), naringenin (**2**), 5,7,3′,5′-tetrahydroxyflavanone (**3**), formononetin (**4**), isoliquiritigenin (**5**), and genistein (**6**) were isolated from the stems of *M. reticulata* Benth. The structures of **1**−**6** were determined by spectroscopic methods. The effects of flavonoid derivatives (**1**−**6**) on the viability of human cancer cells (including HepG2, SK-Hep-1, Huh7, PLC5, COLO 205, HT-29, and SW 872 cells) were investigated. The results indicated that genistein (**6**) had the strongest inhibitory activity with an IC_{50} value of 16.23 μM in SK-Hep-1 human hepatocellular carcinoma cells. Treatment of SK-Hep-1 cells with genistein (**6**) caused loss of mitochondrial membrane potential. Western blot data revealed that genistein (**6**) stimulated an increase in the protein expression of Fas, FasL, and p53. Additionally, treatment with genistein (**6**) changed the ratio of expression levels of pro- and anti-apoptotic Bcl-2 family members and subsequently induced the activation of caspase-9 and caspase-3, which was followed by cleavage of poly(ADP-ribose) polymerase (PARP). These results demonstrate that genistein (**6**) induces apoptosis in SK-Hep-1 cells via both Fas- and mitochondria-mediated pathways.

KEYWORDS: ***Millettia reticulata* Benth; apoptosis; genistein; SK-Hep-1 cells**

INTRODUCTION

Cell death under physiological conditions usually occurs through programmed cell death (apoptosis), and apoptosis plays an important role in anticarcinogenesis. Apoptosis is characterized by the activation of the caspase family of cysteine proteases that is followed by specific caspase-mediated morphological changes including cell shrinkage, chromatin condensation, nuclear DNA fragmentation, membrane blebbing, and breakdown of the cell into apoptotic bodies (*1*). Apoptosis can be activated through two main pathways, which are classified as the mitochondria-dependent pathway (intrinsic pathway) and the death receptor-dependent pathway (extrinsic pathway) (*2*). Mitochondria play an essential role in the permeability of the transition pore opening, and collapse of the mitochondrial membrane potential results in the rapid release of caspase activators (*3*, *4*). Changes in the membrane phosphatidylserine externalization are generally observed at a later stage than the loss of mitochondrial membrane potential (*5*). Many models of apoptosis have demonstrated that disruption of the mitochondrial transmembrane potential (MTP) is mediated by the opening of the mega-channel (permeability transition pore), which precedes caspase activation (*6*).

The stem of *Millettia reticulata* Benth is a member of the Leguminosae/Fabaceae family. *M. reticulata* Benth is cultivated in Malaysia, Indonesia, Burma, China, and Japan. It has multiple biological functions and is one of the oldest tonic herbs in traditional Chinese medicine. It is obtained from several legume shrubs containing red resins and is also called Ji Xue Teng in China. It has been elevated to one of the most commonly used herbs of modern Chinese medicine. Chen et al. (*7*) indicated that *M. reticulata* Benth exhibits pharmacological effects. *Spatholobus suberectus* Dunn is also a member of the Leguminosae family. It has been used in traditional Chinese medicine for rheumatism, anemia, menoxenia, and other disorders. Lee et al. (*8*) demonstrated that flavonoids and derivatives isolated from *S. suberectus* have interesting biological properties. *S. suberectus* has been used as a clinical medicine to treat skin-whitening, menstrual abnormalities, thrombosis, and numbness and has anti-inflammatory activities (*9*−*12*). Our previous studies have shown that water

*Author to whom correspondence should be addressed (telephone 886-4-22879755; fax 886-4-22854378; e-mail gcyen@nchu.edu.tw).

 Published on Web 12/08/2009

extracts of *M. reticulata* Benth possess potent antioxidant and anti-inflammatory efficacy that might be able to protect against liver injury induced by CCl_4 in rats (*13*). Recent studies concerning the bioavailability of polyphenols are in agreement with their potential therapeutic effects. In a bioavailability study (*14*), following oral administration of genistein (6.25, 12.5, and 50 mg/kg), the compound was detected in the plasma, and the C_{max} values at 10 min after administration were 106, 258, and 748 ng/mL, respectively. However, the literature regarding the anticancer activity of flavonoid derivatives isolated and identified from *M. reticulata* Benth remains unclear.

The objectives of this study were to investigate the anticancer effects of flavonoid derivatives isolated and identified from the ethyl acetate extracts of the stems of *M. reticulata* Benth. In the present study, various human cancer cells (HepG2, SK-Hep-1, Huh7, PLC5, COLO 205, HT-29, and SW 872 cells) were used for in vitro evaluation of anticancer activity. The anticancer effects of flavonoid derivatives isolated from the stems of *M. reticulata* Benth on Fas- and mitochondria-mediated pathways in human cancer cells were also investigated.

MATERIALS AND METHODS

Materials. Stems of *M. reticulata* Benth were collected in Taichung, Taiwan, in December 2006. Sodium bicarbonate, MTT dye [3-(4,5-dimethylthiazol-2-yl)-2,5-diphenyltetrazolium bromide], propidium iodide (PI), and 4, 6-diamidino-2-phenylindole dihydrochloride (DAPI) were purchased from Sigma Chemical Co. (St. Louis, MO). Dimethyl sulfoxide (DMSO) was purchased from Merck Co. (Darmstadt, Germany). Dulbecco's modified Eagle's medium, RPMI 1640 medium, Leibovitz's L-15 medium, fetal bovine serum, L-glutamine, nonessential amino acids, sodium pyruvate, and the antibiotic mixture (penicillin−streptomycin) were purchased from Invitrogen Co. (Carlsbad, CA). Anti-β-actin, anti-Bax, anti-Bcl-2, anticaspase-3, anti-Fas, anti-FasL, anti-PARP [poly-(ADP-ribose) polymerase], and anti-p53 antibodies were purchased from Cell Signaling Technology (Beverly, MA). Anticaspase-9 antibody was obtained from BioVision (Mountain View, CA). Anti-rabbit and anti-mouse secondary horseradish peroxidase antibodies were purchased from Bethyl Laboratories (Montgomery, TX). Protein molecular mass markers were obtained from Pharmacia Biotech (Saclay, France). Poly(vinyl difluoride) (PVDF) membranes for Western blotting were obtained from Millipore (Bedford, MA). All other chemicals were of reagent grade.

Extraction and Isolation of Compounds from *Millettia reticulata* Benth. The air-dried stems (5.0 kg) were extracted with methanol (20 L) twice in a percolator and then filtered. The filtrate was evaporated in vacuo to give a dark brown residue, which was suspended in water and partitioned with CH_2Cl_2, EtOAc, and BuOH. The EtOAc extract (41.8 g) was chromatographed by a silica gel (70−230 mesh, Merck) and eluted with *n*-C_6H_{14} gradually enriched with EtOAc, which showed 11 fractions by TLC profile. Fraction 2 eluted with *n*-C_6H_{14}/EtOAc (7:1, v/v) was further fractionated using silica gel column chromatography (230−400 mesh, Merck) by elution with C_6H_6/EtOAc (5:1, v/v) and preparative TLC developing with CH_2Cl_2/EtOAc (5:1, v/v) to obtain (−)-epicatechin (**1**, 8.8 mg) and naringenin (**2**, 8.2 mg). 5,7,3′,5′-Tetrahydroxyflavanone (**3**, 11.6 mg) was obtained from fraction 3 (6.5 g) by means of silica gel column chromatography (230−400 mesh, Merck) by elution with *n*-C_6H_{14}/EtOAc (6:1, v/v) and preparative TLC developing with CH_2Cl_2/EtOAc (4:1, v/v). Fraction 6 (12.7 g) was repeatedly subjected to silica gel column chromatography (230−400 mesh, Merck) by elution with CH_2Cl_2/EtOAc (6:1, v/v) and preparative TLC developing with $CHCl_3$/MeOH (5:1, v/v) to obtain 7-hydroxy-4′-methoxyisoflavone (**4**, 10.5 mg) and 4,2′,4′-trihydroxychalcone (**5**, 10.4 mg). Fraction 8 (7.0 g) was rechromatographed on silica gel (230−400 mesh, Merck) by elution with CH_2Cl_2/EtOAc (4:1, v/v) and preparative TLC developing with $CHCl_3$/MeOH (5:1, v/v) to obtain genistein (**6**, 12.4 mg).

Spectrometry. Optical rotations were measured with a JASCO DIP-370 digital polarimeter (JASCO Ltd., Tokyo, Japan). UV spectra were obtained on a Thermo model α UV−vis spectrophotometer (Thermo Spectronic, Cambridge, U.K.). ^{1}H (400 MHz) and ^{13}C NMR (100 MHz) experiments were performed with a Varian Unity 400 NMR spectrophotometer (Varian, CA). EIMS measurements were performed on a JMS HX-100 mass spectrometer (JEOL Ltd., Tokyo, Japan).

Cell Culture. Human hepatocellular carcinoma cells (Huh7 cells, PLC5 cells, and SK-Hep-1 cells) were obtained from the American Type Culture Collection (ATCC, Bethesda, MD). Human liposarcoma cells (SW 872 cells) and human hepatoblastoma cell (HepG2 cells) were obtained from the Bioresource Collection and Research Center (BCRC, Food Industry Research and Development Institute, Hsinchu, Taiwan). Human colorectal carcinoma cells (COLO 205 cells and HT-29 cells) were provided by Dr. Min-Hsiung Pan (National Kaohsiung Marine University, Kaohsiung, Taiwan). HepG2 cells, PLC5 cells, Huh7 cells, and SK-Hep-1 cells were grown in 90% Dulbecco's modified Eagle's medium supplemented with 10% fetal bovine serum, 2 mM L-glutamine, 1.5 g/L sodium bicarbonate, 0.1 mM nonessential amino acids, 1.0 mM sodium pyruvate, 100 units/mL penicillin, and 100 μg/mL streptomycin. COLO 205 cells and HT-29 cells were grown in 90% RPMI 1640 medium supplemented with 10% fetal bovine serum, 100 units/mL penicillin, and 100 μg/mL streptomycin. SW 872 cells were grown in 90% Leibovitz's L-15 medium supplemented with 10% fetal bovine serum, 100 units/mL penicillin, and 100 μg/mL streptomycin. SW 872 cells were cultured at 37 °C in a humidified atmosphere with free gas exchange without CO_2. Other cells were cultured at 37 °C in a humidified 5% CO_2 incubator.

Cell Viability by MTT Assay. The MTT assay was performed according to the method of Mosmann (*15*). Cancer cells were plated into 96-well microtiter plates at a density of 1×10^4 cells/well. After 24 h, culture medium was replaced by 200 μL serial dilutions (0−100 μM) of compounds **1**−**6**, and the cells were incubated for 48 h. The final concentration of solvent was $<0.1\%$ in cell culture medium. Culture medium was removed and replaced by 90 μL of fresh culture medium. Ten microliters of sterile filtered MTT solution (5 mg/mL) in phosphate-buffered saline (PBS, pH 7.4) was added to each well, thereby reaching a final concentration of 0.5 mg of MTT/mL. After 5 h, unreacted dye was removed, and the insoluble formazan crystals were dissolved in 200 μL/well DMSO and measured spectrophotometrically in a FLUOstar galaxy spectrophotometer (BMG Labtechnologies Ltd., Offenburg, Germany) at 570 nm. The relative cell viability (%) related to control wells containing cell culture medium without samples was calculated as A_{570nm} [sample]/A_{570nm} [control] × 100. The IC_{50} value was calculated as the concentration of compounds **1**−**6** that caused 50% inhibition of cell growth when compared to untreated controls.

Nuclear Staining with PI and DAPI. Apoptosis was evaluated by staining with PI and DAPI. Cells were stimulated with 0−50 μM genistein (**6**) for 48 h. PI stained cells were fixed with 80% ethanol for 30 min and incubated with 40 μg/mL PI solution for 30 min in the dark. DAPI-stained cells were fixed with 4% paraformaldehyde for 30 min and incubated with 1 μg/mL DAPI solution for 30 min in the dark. The nuclear morphology of the cells was examined by fluorescence microscopy (Olympus, Tokyo, Japan). Typical apoptotic changes included chromatin condensation, chromatin compaction along the periphery of the nucleus, and segmentation of the nucleus.

Annexin V-FITC/PI Assay. The annexin V-FITC/PI assay was performed using the annexin V-FITC kit (ANNEX100F, SEROTEC, U. K.) according to the instructions of the manufacturer. Briefly, 1×10^6 cells were plated in a 6 cm dish. Cells were treated with 0−50 μM genistein (**6**) for 48 h. The cells were labeled with annexin V-FITC/PI according to the instructions of the manufacturer. The annexin V-FITC−/PI− population was regarded as normal, healthy cells, whereas annexin V-FITC+/PI− cells were taken as a measure of early apoptosis, annexin V-FITC+/PI+ as late apoptosis, and annexin V-FITC−/PI+ as necrosis. About 1×10^4 events were acquired and analyzed using CELL Quest software.

Mitochondrial Membrane Potential ($\Delta\Psi_m$) Analysis. Mitochondrial membrane potential was determined using the MitoPT 100 test kit (Immunochemistry Technologies, LLC). JC-1 is a cationic dye that exhibits potential-dependent accumulation in mitochondria and indicates a fluorescence emission shift from green to red. Cells were seeded in 12-well plates. After 24 h, the cells were treated with 0−50 μM genistein (**6**) for 6 and 12 h. Routine passage consisted of rinsing cells in 12-well plates once with PBS, followed by harvesting with 0.1 mL of TE solution, addition of 1 mL of fresh culture medium, and thorough dispersion. Aliquots of the resultant cell suspensions were placed in Eppendorf tubes containing 1×10^6 cells per Eppendorf and 1 mL of culture medium. After centrifugation,

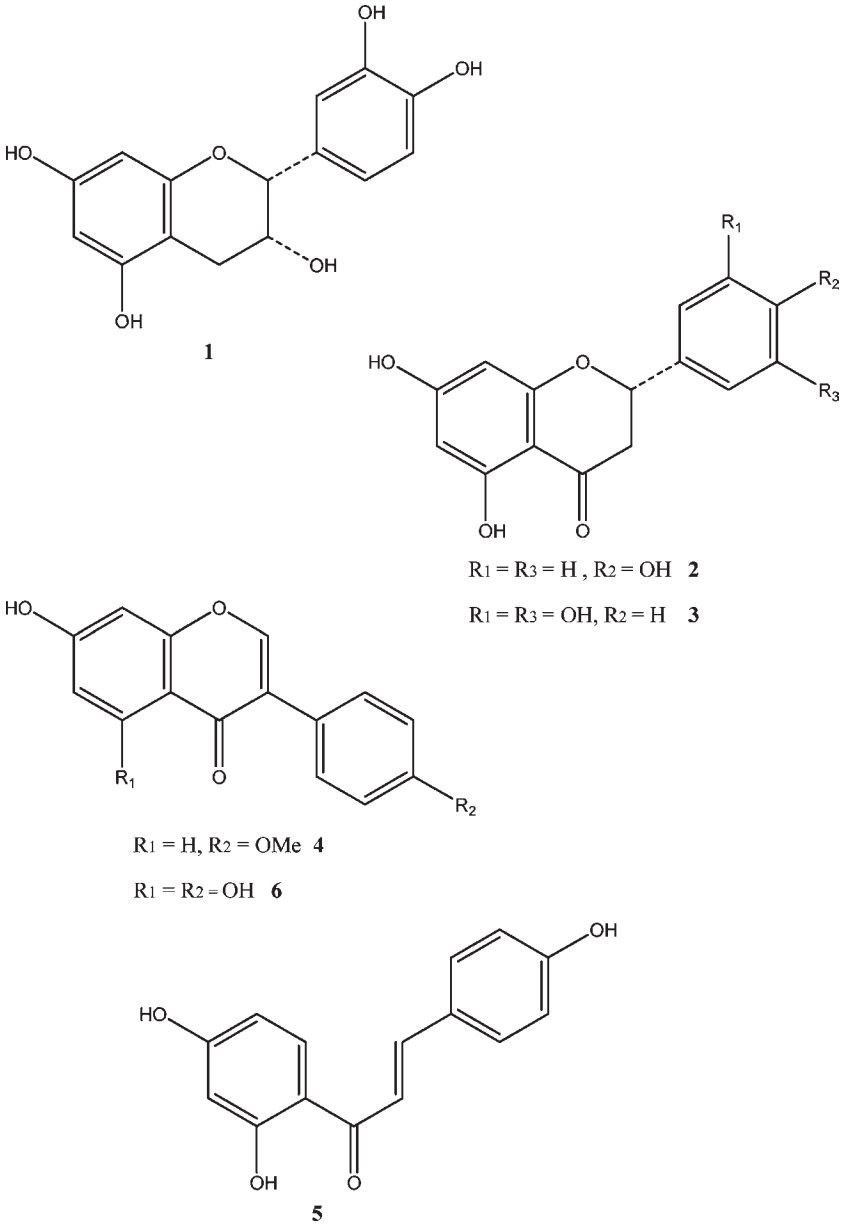

Figure 1. Chemical structures of isolated compounds **1**−**6**.

cells were incubated with 10 μg/mL JC-1 at 37 °C for 15 min in a humidified 5% CO_2 incubator. Cells were collected and washed with 1× assay buffer (MitoPT 100 test kit). The cells were then resuspended in an adequate amount of the same solution and analyzed by a FLUOstar galaxy fluorescence plate reader with an excitation wavelength of 485 nm and an emission wavelength of 590 nm for red fluorescence. Apoptotic cells will generate a lower reading of red fluorescence, and the changes in the mitochondrial membrane potential ($\Delta\Psi_m$) can be most accurately assessed by comparing the red fluorescence of untreated cells and cells treated with genistein (**6**). The morphology of the cells was examined by fluorescence microscopy (Olympus).

Western Blot Analysis. Cells (1×10^7 cells/10 cm dish) were incubated with 0−25 μM genistein (**6**) for 2 and 5 h. Cells were collected and lysed in ice-cold lysis buffer [20 mM Tris-HCl (pH 7.4), 2 mM EDTA, 500 μM sodium orthovanadate, 1% Triton X-100, 0.1% SDS, 10 mM NaF, 10 μg/mL leupeptin, and 1 mM PMSF]. Fas, FasL, p53, Bax, Bcl-2, caspase-9, caspase-3, PARP, and β-actin protein expressions were assessed in SK-Hep-1 cells. The protein concentration of the cell lysate was estimated with the Bio-Rad DC protein assay kit (Bio-Rad Laboratories, Hercules, CA) using bovine serum albumin as the standard. Total protein (50−60 μg) was separated by sodium dodecyl sulfate−polyacrylamide gel electrophoresis (SDS-PAGE) using a 12% polyacrylamide gel. The proteins in the gel were transferred to a PVDF membrane. The membrane was blocked with 5% skim milk in PBST (0.05% v/v Tween-20 in PBS, pH 7.2) for 1 h. Membranes were incubated with primary antibody (1:5000) at 4 °C overnight and then with secondary antibody (1:5000) for 1 h. Membranes were washed three times in PBST for 10 min between each step. The signal was detected using the Amersham ECL system (Amersham-Pharmacia Biotech, Arlington Heights, IL). Relative protein expression was quantified densitometrically using LabWorks 4.5 software and calculated according to the β-actin reference bands.

Statistical Analysis. Statistical analysis was performed using SAS software. Analyses of variance were performed using ANOVA procedures. Significant differences ($p < 0.05$) between the means were determined by Duncan's multiple-range tests. Each treatment was performed in triplicate.

RESULTS AND DISCUSSION

Isolation and Identification of Flavonoid Derivatives from *Millettia reticulata* Benth. The EtOAc-soluble fraction of the stems of *M. reticulata* Benth led to the isolation of one flavan-3-ol (**1**), two flavanone (**2** and **3**), two isoflavone (**4** and **6**), and one chalcone (**5**) derivative. The structures of the six compounds

Table 1. Effects of Compounds **1**−**6** Isolated from *Millettia reticulata* Benth on the Cell Viability of Human Cancer Cells

	IC_{50}[a] (μM)					
cell line	**1**	**2**	**3**	**4**	**5**	**6**
HepG2	−[b]	−	−	−	−	20.29 ± 0.61
SK-Hep-1	−	23.12 ± 1.17	18.28 ± 2.30	95.90 ± 7.29	19.08 ± 3.90	16.23 ± 0.30
Huh7	−	−	62.40 ± 8.00	−	−	18.67 ± 0.66
PLC5	−	−	87.07 ± 6.10	−	−	18.55 ± 0.65
COLO 205	−	20.95 ± 1.08	23.62 ± 2.49	−	−	20.20 ± 1.24
HT-29	−	17.98 ± 0.73	−	−	−	17.51 ± 0.65
SW 872	−	−	20.92 ± 1.37	−	−	19.59 ± 1.04

[a] Cells were treated with 0−100 μM compounds **1**−**6** for 48 h. The reported values are the means ± SD (n = 3). [b] The IC_{50} value was >100 μM.

(**Figure 1**) were identified by comparing their physical and spectroscopic data (UV, ^{1}H NMR, ^{13}C NMR, and EIMS) with those of reported values.

Compound (**1**): $[\alpha]_D$ −15.4°. The ^{1}H NMR spectrum of **1** revealed the presence of a methylene proton, two oxymethine protons, two meta-coupled aromatic protons in the A-ring, and an ABX type aromatic proton in the B-ring. The ^{13}C NMR spectrum of **1** showed 15 carbon signals. The EIMS of **1** showed a $[M]^+$ at m/z 290. From the above results, formula **1** was proposed for the structure of (−)-epicatechin. The chemical shifts of this compound matched the reported values (*16*).

Compound (**2**): naringenin was a yellow amorphous powder. The UV spectrum exhibited maxima at 264 and 320 nm. The ^{1}H NMR spectrum of **2** revealed the presence of one methylene α to the carbonyl at δ 3.09 (dd, J = 17.0, 13.0 Hz, H_{ax}-3) and δ 2.74 (dd, J = 17.0, 2.6 Hz, H_{eq}-3) and one oxymethine δ 5.32 (dd, J = 13.0, 2.6 Hz, H-2). These data suggested that **2** had a flavanone skeleton. Furthermore, the ^{1}H NMR spectrum exhibited the presence of an A_2B_2 type aromatic proton and two meta-coupled aromatic protons. The ^{13}C NMR spectrum of **2** showed 15 carbon signals. The EIMS of **2** showed a $[M]^+$ at m/z 272. From the above results, formula **2** was proposed for the structure of naringenin. The chemical shifts of this compound matched the reported values (*17*). Comparison of the ^{1}H NMR spectrum of **3** with that of **2** revealed that **3** has the same flavanone skeleton. From the EIMS and ^{13}C NMR spectral data, the structure of **3** was established as 5,7,3′,5′-tetrahydroxyflavanone. The chemical shifts of this compound matched the reported values (*18*).

Compound (**4**) was a yellow amorphous powder. The UV spectrum exhibited maxima at 265 and 322 (sh) nm. The ^{1}H NMR spectrum of **4** revealed the presence of A_2B_2 type aromatic protons in the B-ring, an ABX type aromatic proton in the A-ring, and a singlet proton at δ 7.86. The EIMS and ^{13}C NMR spectral data established the structure of compound **4** as 7-hydroxy-4′-methoxyisoflavone; this was identical with formononetin, which has previously been reported (*19*).

The EIMS, ^{1}H, and ^{13}C NMR spectral data established the structures of compounds **5** and **6** as 4,2′,4′-trihydroxy chalcone and 5,7,4′-trihydroxyisoflavone, which were identical with isoliquiritigenin and genistein, respectively, which have also previously been reported (*20*, *21*).

Effects of Flavonoid Derivatives on Cell Population Growth. To assess whether these six flavonoid derivatives isolated from the stems of *M. reticulata* Benth could inhibit the population growth of cells, HepG2, SK-Hep-1, Huh7, PLC5, COLO 205, HT-29, and SW 872 human cancer cells were treated with 0−100 μM compounds **1**−**6**, and population growth was determined via MTT assay. **Table 1** shows that among the six flavonoid derivatives tested, genistein (**6**) had the strongest population growth inhibition of SK-Hep-1 human hepatocellular carcinoma cells. Moreover, the 50% inhibitory concentration (IC_{50}) as determined by MTT assay after 48 h of incubation showed the highest activity for genistein (**6**) with an IC_{50} value of 16.23 μM. Many studies have demonstrated that genistein induces apoptosis in cancer cells such as MCF-7, HT-29, HepG2, and HL-60 cells (*22*−*25*). Therefore, genistein (**6**) was selected for all subsequent studies.

Genistein (6)-Induced Apoptosis in SK-Hep-1 Cells. Figure 2 shows the effect of genistein (**6**) on percentage of normal, early apoptotic, late apoptotic, and necrotic SK-Hep-1 cells. These results indicated that treatment with 0−50 μM genistein (**6**) decreased the number of viable SK-Hep-1 cells in a dose-dependent manner. The apoptotic cells, including early apoptotic (annexin V-FITC+/PI−) and late apoptotic cells (annexin V-FITC+/PI+), were increased in a dose-dependent manner. Kim et al. (*23*) have previously shown that genistein inhibits the viability of HT-29 cells in a dose-dependent manner. Classical apoptotic cells were identified after genistein (**6**) treatment by identification of cell shrinkage, membrane blebbing, and apoptotic body formation (**Figure 3A**). The nuclear morphology of untreated and treated cells stained with PI and DAPI is shown in panels **B** and **C**, respectively, of **Figure 3**. PI and DAPI staining showed apoptotic bodies when cells were treated with 50 μM genistein (**6**) for 48 h. Chodon et al. (*24*) showed that nuclear condensation and formation of apoptotic bodies occur when HepG2 cells are treated with 16 μM genistein for 24 and 48 h.

Disruption of Mitochondria Membrane Potential ($\Delta\Psi_m$) in Cells Treated with Genistein (6). Alterations in mitochondrial function have been shown to play a crucial role in apoptosis, and thus the effect of genistein (**6**) on the mitochondrial membrane potential was investigated. In this assay, nonapoptotic cells with healthy mitochondria had red fluorescence and apoptotic cells had green fluorescence. SK-Hep-1 cells showed a significant ($p < 0.05$) decrease in red fluorescence intensity when treated with 0−50 μM genistein (**6**) for 6 and 12 h (**Figure 4**). These results demonstrate early damage to mitochondria membrane potential, which may further activate the intrinsic pathway of apoptosis. Sánchez et al. (*25*) demonstrated that genistein induces apoptosis in HL-60 cells through reactive oxygen species-inducible protein kinases. Yeh et al. (*26*) demonstrated that genistein induces apoptosis of Hep3B cells by disruption of mitochondria membrane potential.

Genistein (6) Induces Apoptosis via a Fas- and Mitochondrial-Mediated Pathway. Cancer prevention has become an important approach to control cancer. Apoptosis may be initiated through the regulation of death receptors located on the cell surface or through an intrinsic pathway, which includes the release of apoptotic signals from the mitochondria (*27*). The effect of genistein (**6**) on the constitutive protein levels of Fas, FasL, and p53 in SK-Hep-1 cells is shown in **Figure 5**. Genistein (**6**) (25 μM, 5 h) resulted in a significant increase in Fas and FasL expression from 1.00 (control) to 1.19- and 1.42-fold, respectively. Treatment of cells with genistein (**6**) (5 μM, 5 h) also significantly increased p53 expression from 1.00 (control) to 1.65-fold. The Bcl-2 family plays a crucial role in apoptosis because it includes both

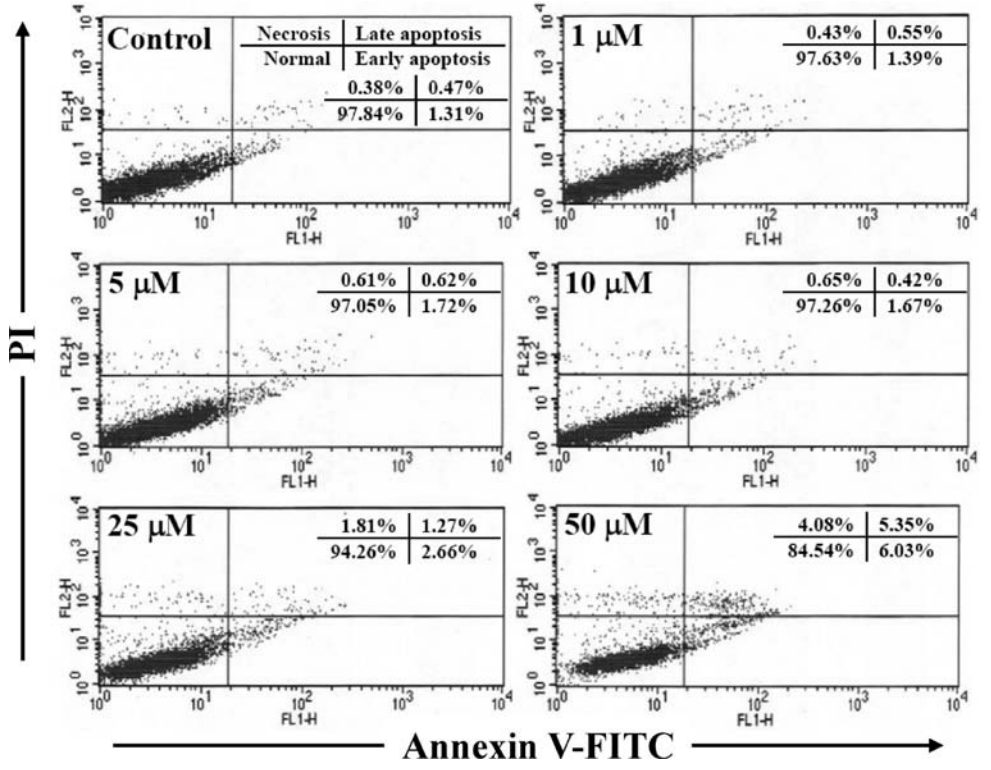

Figure 2. Flow cytometric analysis of genistein (**6**)-mediated cell apoptosis in SK-Hep-1 cells (annexin V-FITC/PI double-stained cells). Cells were treated with 0−50 μM genistein (**6**) for 48 h. The percentage of apoptotic/necrotic cells was calculated by CELL Quest software (mean ± SD, $n = 3$).

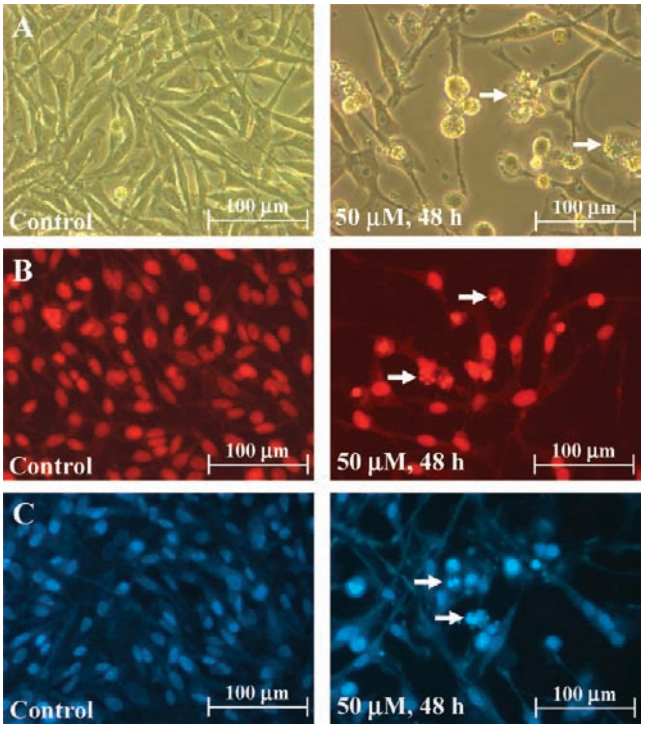

Figure 3. Effect of genistein (**6**) on cell morphology of SK-Hep-1 cells: (**A**) unstained; (**B**) cells stained with PI; (**C**) cells stained with DAPI. Cells were treated with 0−50 μM genistein (**6**) for 48 h.

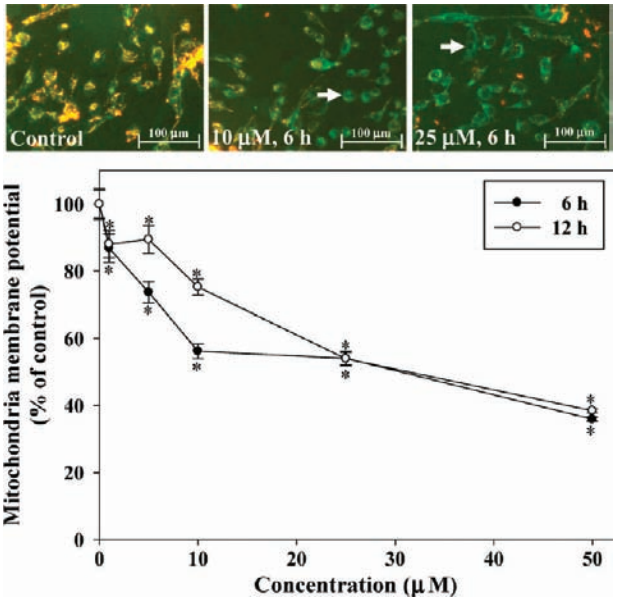

Figure 4. Effect of genistein (**6**) on mitochondria membrane potential ($\Delta\Psi_m$) in SK-Hep-1 cells. Cells were treated with 0−50 μM genistein (**6**) for 6 and 12 h. Reported values are the mean ± SD ($n = 3$). *, significantly different from control ($p < 0.05$).

anti-apoptotic members such as Bcl-2 and pro-apoptotic members such as Bax (*28*). **Figure 6** shows the effect of genistein (**6**) on the protein expression of Bax and Bcl-2 and the Bax/Bcl-2 ratio in SK-Hep-1 cells. The pro-apoptotic protein expression of Bax was increased from 1.00 (control) to 3.51-fold after treatment with 25 μM genistein (**6**) for 2 h. The anti-apoptotic protein expression of Bcl-2 was decreased from 1.00 (control) to 0.84-fold after treatment with 25 μM genistein (**6**) for 5 h. Many studies have indicated that genistein induces apoptosis in human hepatocellular carcinomas and MCF-7 cells through the Bcl-2 family pathway (*22*, *26*). Moreover, the ratio of Bax/Bcl-2 is a decisive factor that plays an important role in determining whether cells will undergo apoptosis under experimental conditions that promote cell death (*29*). A significant dose-dependent shift in the

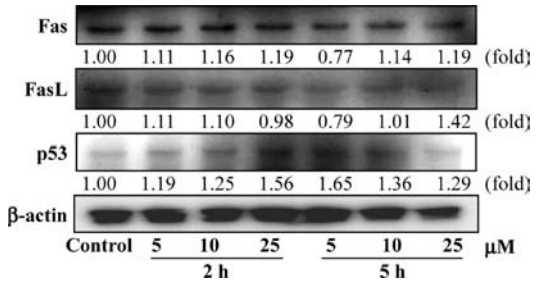

Figure 5. Effect of genistein (**6**) on expression of Fas, FasL, and p53 in SK-Hep-1 cells. Cells were treated with 0−25 μM genistein (**6**) for 2 and 5 h. Relative protein expression was quantified densitometrically using LabWorks 4.5 software and calculated according to the β-actin reference bands.

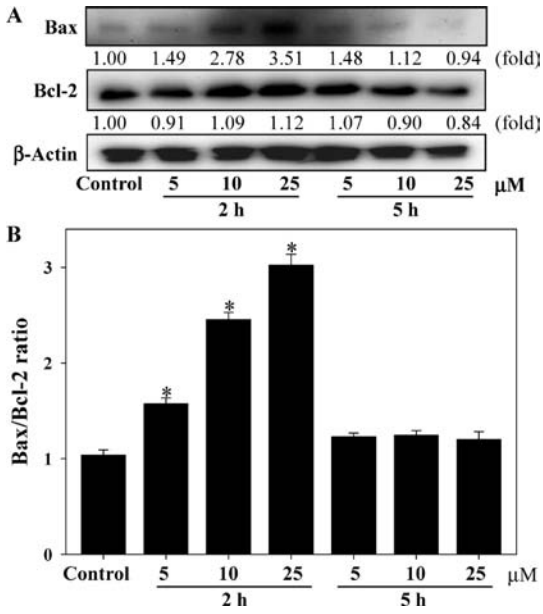

Figure 6. Effect of genistein (**6**) on expression of Bax and Bcl-2 (**A**) and the Bax/Bcl-2 ratio (**B**) in SK-Hep-1 cells. Cells were treated with 0−25 μM genistein (**6**) for 2 and 5 h. Relative expression was quantified densitometrically using LabWorks 4.5 software and calculated according to the β-actin reference bands.

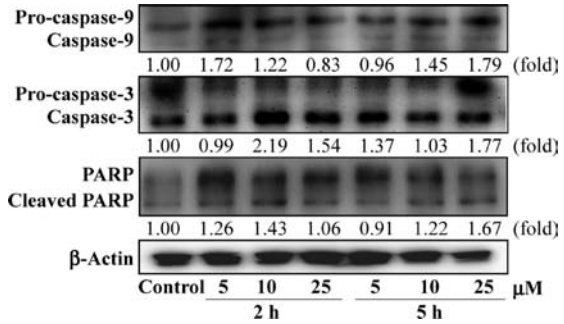

Figure 7. Effect of genistein (**6**) on expression of caspase-9, caspase-3, and PARP in SK-Hep-1 cells. Cells were treated with 0−25 μM genistein (**6**) for 2 and 5 h. Relative protein expression was quantified densitometrically using LabWorks 4.5 software and calculated according to the β-actin reference bands.

ratio of Bax and Bcl-2 was observed after cells were treated with 0−25 μM genistein (**6**) for 2 h, indicating the induction of the apoptotic process (**Figure 6B**). As shown in **Figure 7**, treatment of SK-Hep-1 cells with genistein (**6**) revealed the activation of caspase-9 and caspase-3. Caspase-3 cleaves PARP, which leads to DNA fragmentation and ultimately to apoptosis (*30*). Treatment of cells with genistein (**6**) induced PARP cleavage: the maximal degradation was 1.67-fold, which occurred after treatment with 25 μM genistein (**6**) for 5 h (**Figure 7**). These results were further confirmed upon monitoring the cleavage of PARP, which is targeted by active caspase-3 (*31*). Our results are consistent with previous studies. Oh et al. (*32*) indicated that ginsenoside-Rh2 induces apoptosis in SK-Hep-1 cells via mitochondrial pathway. Jung et al. (*33*) indicated that allylthiopyridazine derivatives induce apoptosis in SK-Hep-1 cells via a caspase-3-dependent pathway.

In conclusion, the present study showed that genistein (**6**) isolated from the stems of *M. reticulata* Benth led to loss of mitochondrial transmembrane potential; increased protein expression of Fas, FasL, and p53; regulation of Bcl-2 family members; and subsequent activation of caspases followed by cleavage of PARP. These results provide a potential molecular mechanism for genistein (**6**)-induced apoptosis in SK-Hep-1 human hepatocellular carcinoma cells and suggest that the stems of *M. reticulata* Benth may provide a health benefit for humans. Moreover, the anticancer effects of other potential compounds from the stems of *M. reticulata* Benth in human hepatocellular carcinoma cells may also have potential for anticancer applications.

ABBREVIATIONS USED

DAPI, 4,6-diamidine-2-phenylindole; DMSO, dimethyl sulfoxide; IC_{50}, 50% inhibitory concentration; $\Delta\Psi_m$, mitochondria membrane potential; MTT, 3-(4,5-dimethylthiazol-2-yl)-2,5-diphenyltetrazolium bromide; PARP, poly(ADP-ribose) polymerase; PBS, phosphate-buffered saline; PI, propidium iodide; PVDF, poly(vinyl difluoride); SDS-PAGE, sodium dodecyl sulfate−polyacrylamide gel electrophoresis.

LITERATURE CITED

(1) Johnstone, R. W.; Ruefli, A. A.; Lowe, S. W. Apoptosis: a link between cancer genetics and chemotherapy. *Cell* **2002**, *108*, 153–164.

(2) Thornberry, N. A.; Rano, T. A.; Peterson, E. P.; Rasper, D. M.; Timkey, T.; Garcia-Calvo, M.; Houtzager, V. M.; Nordstrom, P. A.; Roy, S.; Vaillancourt, J. P.; Chapman, K. T.; Nicholson, D. W. A combinatorial approach defines specificities of members of the caspase family and granzyme B. Functional relationships established for key mediators of apoptosis. *J. Biol. Chem.* **1997**, *272*, 17907–17911.

(3) Li, P.; Nijhawan, D.; Budihardjo, J.; Srinivasula, S. M.; Ahmad, M.; Alnewri, E. S.; Wang, X. Cytochrome *c* and ATP-dependent formation of Apaf-1/caspase-9 complex initiates an apoptotic proteasome cascade. *Cell* **1997**, *91*, 479–489.

(4) Green, D. R.; Reed, J. C. Mitochondria and apoptosis. *Science* **1998**, *281*, 1309–1312.

(5) Raghuvar Gopal, D. V.; Narkar, A. A.; Badrinath, Y.; Mishra, K. P.; Joshi, D. S. Protection of Ewing's sarcoma family tumor (ESFT) cell line SK-N-MC from betulinic acid induced apoptosis by *R*-DL-tocopherol. *Toxicol. Lett.* **2004**, *153*, 201–212.

(6) Zamzami, N.; Metivier, D.; Kroemer, G. Quantitation of mitochondrial transmembrane potential in cells and isolated mitochondria. *Methods Enzymol.* **2000**, *322*, 208–213.

(7) Chen, Y. P.; Chen, C. C.; Hsu, H. Y. Pharmacological activities of the flavonoids of *Bauhinia championii* and *Millettia reticulata*. *Prog. Clin. Biol. Res.* **1986**, *213*, 297–300.

(8) Lee, M. H.; Lin, Y. P.; Hsu, F. L.; Zhan, G. R.; Yen, K. Y. Bioactive constituents of *Spatholobus suberectus* in regulating tyrosinase-related proteins and mRNA in HEMn cells. *Phytochemistry* **2006**, *67*, 1262–1270.

(9) Cheng, J.; Liang, H.; Wang, Y.; Zhao, Y. Y. Studies on the constituents from the stems of *Spatholobus suberectus*. *Zhongguo Zhong Yao Za Zhi* **2003**, *28*, 1153–1155.

(10) Lee, J. Y.; Kang, W. H. Effect of cyclosporine A on melanogenesis in cultured human melanocytes. *Pigment Cell Res*. **2003**, *16*, 504–508.
(11) Li, R. W.; David Lin, G.; Myers, S. P.; Leach, D. N. Anti-inflammatory activity of Chinese medicinal vine plants. *J. Ethnopharmacol*. **2003**, *85*, 61–67.
(12) Chen, D. H.; Luo, X.; Yu, M. Y.; Zhao, Y. Q.; Cheng, Y. F.; Yang, Z. R. Effect of *Spatholobus suberectus* on the bone marrow cells and related cytokines of mice. *Zhongguo Zhong Yao Za Zhi* **2004**, *29*, 352–355.
(13) Hsu, C. C.; Hsu, C. L.; Tsai, S. E.; Fu, T. Y.; Yen, G. C. Protective effect of *Millettia reticulata* Benth against CCl(4)-induced hepatic damage and inflammatory action in rats. *J. Med. Food* **2009**, *12*, 821–828.
(14) Zhou, S.; Hu, Y.; Zhang, B.; Teng, Z.; Gan, H.; Yang, Z.; Wang, Q.; Huan, M.; Mei, Q. Dose-dependent absorption, metabolism, and excretion of genistein in rats. *J. Agric. Food Chem*. **2008**, *56*, 8354–8359.
(15) Mosmann, T. Rapid colorimetric assay for cellular growth and survival: application to proliferation and cytotoxicity assays. *J. Immunol. Methods* **1983**, *65*, 55–63.
(16) Nunes, D. S.; Haag, A.; Bestmann, H. J. Two proanthocyanidins from the bark of *Dalbergia monetaria*. *Phytochemistry* **1989**, *28*, 2183–2186.
(17) Yoshinari, K.; Shimazaki, N.; Sashida, Y.; Mimaki, Y. Flavanone xyloside and lignans from *Prunus jamasakura* bark. *Phytochemistry* **1990**, *29*, 1675–1678.
(18) Zheng, Z. P.; Cheng, K. W.; Chao, J.; Wu, J.; Wang, M. Tyrosinase inhibitors from paper mulberry (*Broussonetia papyrifera*). *Food Chem*. **2008**, *106*, 529–535.
(19) Herath, H. M. T. B.; Dassanayake, R. S.; Priyadarshani, M. A.; Silva, S. D.; Wannigama, G. P. Isoflavonoids and a pterocarpan from *Gliricidia sepium*. *Phytochemistry* **1998**, *47*, 117–119.
(20) Takasugi, M.; Niino, N.; Nagao, S.; Anetai, M.; Masamune, T.; Shirata, A.; Takahashi, K. Eight minor phytoalexins from diseased paper mulberry. *Chem. Lett*. **1984**, *13*, 689–692.
(21) Khalid, S. A.; Gellert, M.; Szendrei, K.; Duddeck, H. Prunetin-5-*O*-*β*-D-glucopyranoside, an isoflavone from the peduncle of *Prunus avium* and *P. cerasus*. *Phytochemistry* **1989**, *28*, 1560–1561.
(22) Po, L. S.; Wang, T. T.; Chen, Z. Y.; Leung, L. K. Genistein-induced apoptosis in MCF-7 cells involves changes in Bak and Bcl-x without evidence of anti-oestrogenic effects. *Br. J. Nutr*. **2002**, *88*, 463–469.
(23) Kim, E. J.; Shin, H. K.; Park, J. H. Genistein inhibits insulin-like growth factor-I receptor signaling in HT-29 human colon cancer cells: a possible mechanism of the growth inhibitory effect of genistein. *J. Med. Food* **2005**, *8*, 431–438.
(24) Chodon, D.; Ramanurty, N.; Sakthisekaran, D. Preliminary studies on induction of apoptosis by genistein on HepG2 cell line. *Toxicol. In Vitro* **2007**, *21*, 887–891.
(25) Sánchez, Y.; Amrán, D.; Fernández, C.; de Blas, E.; Aller, P. Genistein selectively potentiates arsenic trioxide-induced apoptosis in human leukemia cells via reactive oxygen species generation and activation of reactive oxygen species-inducible protein kinases (p38-MAPK, AMPK). *Int. J. Cancer* **2008**, *123*, 1205–1214.
(26) Yeh, T. C.; Chiang, P. C.; Li, T. K.; Hsu, J. L.; Lin, C. J.; Wang, S. W.; Peng, C. Y.; Guh, J. H. Genistein induces apoptosis in human hepatocellular carcinomas via interaction of endoplasmic reticulum stress and mitochondrial insult. *Biochem. Pharmacol*. **2007**, *73*, 782–792.
(27) Vermeulen, K.; Van Bockstaele, D. R.; Berneman, Z. N. Apoptosis: mechanisms and relevance in cancer. *Ann. Hematol*. **2005**, *84*, 627–639.
(28) Hunt, A.; Evan, G. Apoptosis. Till death us do part. *Science* **2001**, *293*, 1784–1785.
(29) Merry, D. E.; Korsmeyer, S. J. Bcl-2 gene family in the nervous system. *Annu. Rev. Neurosci*. **1997**, *20*, 245–267.
(30) Salvesen, G. S.; Dixit, V. M. Caspases: intracellular signaling by proteolysis. *Cell* **1997**, *91*, 443–446.
(31) Debatin, K. M.; Krammer, P. H. Death receptors in chemotherapy and cancer. *Oncogene* **2004**, *23*, 2950–2966.
(32) Oh, J. I.; Chun, K. H.; Joo, S. H.; Oh, Y. T.; Lee, S. K. Caspase-3-dependent protein kinase C delta activity is required for the progression of ginsenoside-Rh2-induced apoptosis in SK-HEP-1 cells. *Cancer Lett*. **2005**, *230*, 228–238.
(33) Jung, M. Y.; Kwon, S. K.; Moon, A. Chemopreventive allylthiopyridazine derivatives induce apoptosis in SK-Hep-1 hepatocarcinoma cells through a caspase-3-dependent mechanism. *Eur. J. Cancer* **2001**, *37*, 2104–2110.

Received for review September 11, 2009. Revised manuscript received November 12, 2009. Accepted November 16, 2009. This research work was partially supported by the Council of Agriculture, Republic of China, under Grant 98AS-3.1.3-FD-Z1(1).